Electronic supplementary materials *Mendeleev Commun.*, 2026, **36**, 85–87

Sodium intercalation into the NaNbTi(PO_4)$_3$ NASICON-type phosphate

Ilia R. Cherkashchenko, Rodion V. Panin, Varvara A. Razuvaeva, Alexey O. Polevik, Daniil A. Novichkov, Ivan V. Mikheev, Evgeny V. Antipov and Nellie R. Khasanova

Table of Contents

Experimental S2
  Synthesis of NaNbTi(PO_4)$_3$ S2
  Materials characterization. S2
  Elemental analysis S2
  Crystal structure refinement S2
  XANES measurements S3
  Electrochemical measurements S3
Figure S1 Thermogravimetric curve for the NaNbTi(PO_4)$_3$/C sample S4
Table S1 Structural parameters obtained from Rietveld refinement for NaNbTi(PO_4)$_3$ S4
Table S2 Selected interatomic distances for the NaNbTi(PO_4)$_3$ structure S4
Figure S2 Galvanostatic charge-discharge curves of NaNbTi(PO_4)$_3$ S5
Figure S3 CV curves of NaNbTi(PO_4)$_3$ S5
Table S3 Unit cell parameters for the NaNbTi(PO_4)$_3$ electrodes S6
References S6

Experimental

Synthesis of NaNbTi(PO$_4$)$_3$. In the typical synthetic procedure 12.534 mmol (1.4418 g) of $NH_4H_2PO_4$ (RusChim), 2.089 mmol (0.2799 g) of $Na_2C_2O_4$ (Sigma-Aldrich), and 4.178 mmol (1.8652 g) of $NH_4[NbO(C_2O_4)_2]\cdot 8H_2O$ (Sigma-Aldrich) were separately dissolved in deionized water (25 ml for each reagent). 4.178 mmol (0.2000 g) of titanium metal (50 nm, Merck) was treated by the mixture of NH_3 (25%, 7 ml) and H_2O_2 (30%, 20 ml) solutions upon careful heating to provide the formation of a soluble peroxocomplex. To form a chelating polymer matrix, 10 g of citric acid monohydrate $C_6H_8O_7\cdot H_2O$ were melted and then mixed with the 10 ml of a 5% aqueous suspension of polyvinyl alcohol $(C_2H_4O)_n$. The gel obtained after water evaporation was carbonized by calcination in an open cup. The resulting black amorphous powder was preheated (12 h at 400ºC) in an argon atmosphere and ball-milled in ethanol (2 h at 350 min^{-1}). The obtained precursor was subjected to spark plasma sintering (SPS), which is often used to prepare NASICON-structured materials.[S1] The Labox-625 device (SinterLand, Japan) was employed for the SPS procedure. The powder samples (m ~ 400 mg) were placed in a graphite die (with an inner diameter of 10 mm), which was heated up to 800^{o}C for 3 minutes and held at this temperature for 10 minutes followed by cooling down to room temperature at zero power for 10 minutes. The temperature was controlled with a Chino IR-AH pyrometer focused on the surface of a graphite die. The sintering was carried out in a vacuum (~5 Pa), and a uniaxial stress of 70 MPa was applied.

Materials characterization. The phase composition of the samples and the electrodes (*ex situ*) was analyzed using X-ray powder diffraction (XRPD) data collected on a Huber Guinier G670 camera (transmission mode, Image Plate detector, CuKα_1 radiation $\lambda = 1.54051$ Å, curved Ge (111) monochromator, 3–100º 2θ angular range, 0.03º s^{-1} scanning rate).

The morphology of the samples was investigated using a scanning electron microscope, JEOL JSM – 6390 LA, with a built-in X-ray analyzer, EX-230. The samples were mounted on a holder by a conductive carbon tape. The accelerating voltage of the electron gun was 5–20 kV, images were acquired using primary electrons.

Thermogravimetric (TG) study was performed on a Netzsch STA 449C thermal analyzer within the temperature range of 25–800ºC in the artificial air (20% O_2(g) + 80% Ar(g)) atmosphere, with a heating rate of 5ºC min^{-1}.

Elemental analysis. Elemental analysis was performed using an Agilent 720 ICP-OES spectrometer (Agilent, Mulgrave, Australia). A weighted ~30 mg portion of the analyzed sample was placed in a 50 ml polypropylene (PP) Falcon tube, and concentrated, highly purified acids HNO_3, HCl, and HF were added in the following amounts: 5 ml, 5 ml, and 1 ml, respectively. The sample was vortexed for 1 min and left to stand for 48 hours. Finally, 25 ml of deionized water was added to the top. Before analysis, the sample was further diluted by a factor of 10 or 100, depending on the required concentration.

The calibration standards for Na, Ti, and P were prepared in the range of 0.01 to 100 ppm, while for Nb, it was between 0.01 to 10 ppm. The analytical lines were used in accordance with the recommendation of N. Soltapur *et. al.*[S2] Next, measurements from the following two samples were averaged. A 20 ppm Sc solution (in 5% HNO_3) was used to improve the reproducibility of the results, and accuracy was estimated by standard addition methods.

Crystal structure refinement. Rietveld refinement was carried out with the atomic coordinates of the NASICON-type $NaCrNb(PO_4)_3$ phosphate as the initial structural model. Polynomial and pseudo-Voight functions were used to approximate the background and peak shape profiles, respectively. The deviation of the Na1 site occupancy from the stoichiometric value (Table S1) is typical for NASICON-structured phases and results from high mobility of sodium ions within this framework.[S3] The 8-fold Na2 position (18*c*) was found to be vacant based on a difference Fourier analysis. The (Nb/Ti)O_6 octahedra occurred to be nearly regular, with the metal-oxygen distances of 1.94–1.98 Å (Table S2).

XANES measurements. Nb *K*-edge XANES data were registered in the *ex situ* mode on a laboratory spectrometer from the Department of Radiochemistry, Moscow State University (Moscow, Russia). The spectrometer is based on the Rowland circle geometry (d = 0.5 m) and equipped by X-ray tube with silver anode and silicon drift detector (SDD; Amptek Inc.).[S4] The spherical beam (r = 2.5 mm) was focused by curved Ge monochromator (reflections 12 12 0) to collect Nb *K*-edge XANES spectra in the energy range of 18900−19100 eV. The data were collected in reflection mode. Each spectrum consists of ten spectra, combined and normalized using the IFEFFIT program.[S5]

Electrochemical measurements. The electrochemical measurements were carried out using Swagelok-type two electrode cells with aluminum and stainless-steel current collectors, glass-fiber separators, and sodium metal as a counter electrode. 1 M $NaPF_6$ (Macklin) solution in 1:1 vol. ethylene carbonate (EC) : diethyl carbonate (DEC) (Sigma Aldrich) was served as electrolyte. The working electrodes were prepared by mixing $NaNbTi(PO_4)_3$ material, Super P carbon black, and polyvinylidene difluoride (PVDF, Solef 5130, Solvay S.A.) in a weight ratio of 85:5:10 with *N*-methyl-2-pyrrolidone (NMP, Acros Organics) acting as a solvent. The homogenous slurry was cast on aluminum foil using the Doctor Blade technique and dried overnight. It was then rolled and punched into 15 mm discs that were dried again overnight at 100°C under dynamic vacuum ($p < 10^{-2}$ atm). Electrochemical cells were assembled in a glove box filled with argon (MBraun, $pO_2 < 0.1$ ppm, $pH_2O < 0.1$ ppm).

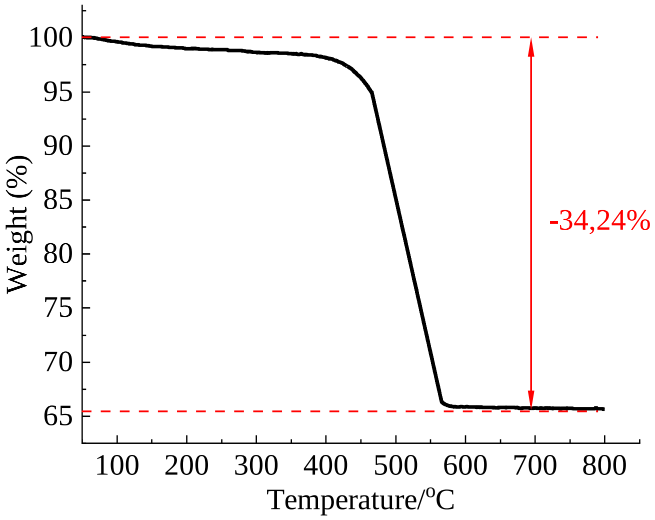

Figure S1 Thermogravimetric curve for the $NaNbTi(PO_4)_3$/C sample (artificial air atmosphere).

Table S1 Structural parameters obtained from Rietveld refinement for $NaNbTi(PO_4)_3$.

Atom	Position	Occupancy	*x/a*	*y/b*	*z/c*	U_{iso}, Å^2
Na1	6*b*	0.862(3)	0	0	0	0.042(1)
Nb1/Ti1	12*c*	0.5Nb/0.5Ti	0	0	0.14552(2)	0.0085(2)
P1	18*e*	1	0.2881(1)	0.2881(1)	0.25	0.0119(4)
O1	36*f*	1	0.4751(1)	0.3079(2)	0.24397(8)	0.0109(3)
O2	36*f*	1	0.1992(2)	0.1756(2)	0.30581(6)	0.0109(3)

Table S2 Selected interatomic distances for the $NaNbTi(PO_4)_3$ structure.

Bond	Distance, Å
Na(1) – O(1)	6×2.512(2)
Nb(1)/Ti(1) – O(1)	3×1.985(1)
Nb(1)/Ti(1) – O(2)	3×1.944(1)
P(1) – O(1)	2×1.533(2)
P(1) – O(2)	2×1.518(1)

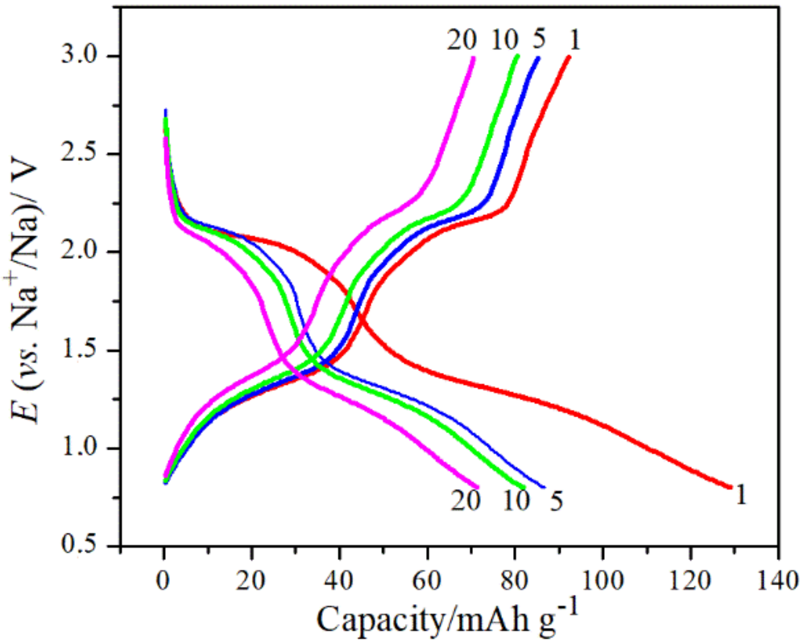

Figure S2 Galvanostatic charge-discharge curves of NaNbTi$(PO_4)_3$ at C/10 rate. Cycle numbers are given.

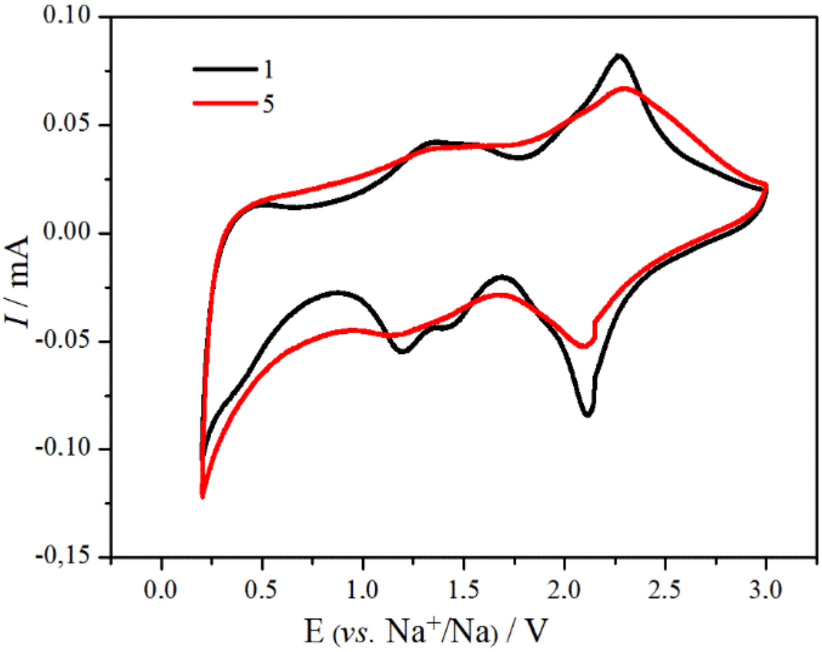

Figure S3 CV curves of NaNbTi$(PO_4)_3$ measured at 0.1 mV s^{-1}. Cycle numbers are given.

Table S3 Unit cell parameters for the $NaNbTi(PO_4)_3$ electrodes: pristine, charged at 0.8 V and discharged at 3.0 V (*vs*. Na^+/Na).

Electrode	*a*, Å	*c*, Å	*V*, $Å^3$
Initial	8.5841(3)	22.110(1)	1410.92(8)
Charged (0.8 V)	8.824(2)	22.197(6)	1496.7(7)
Discharged (3.0 V)	8.5961(9)	22.131(3)	1416.2(3)

References

S1 A. I. Orlova, *J. Nucl. Mater.*, 2022, **559**, 153407; https://doi.org/10.1016/j.jnucmat.2021.153407.

S2 P. N. Soltanpour, G. W. Johnson, S. M. Workman, J. B. Jones, Jr. and R. O. Miller, in *Methods of Soil Analysis: Part 3 Chemical Methods*, eds. D. L. Sparks, A. L. Page, P. A. Helmke, R. H. Loeppert, P. N. Soltanpour, M. A. Tabatabai, C. T. Johnston and M. E. Sumner, Soil Science Society of America, Madison, WI, 1996, pp. 91–139; https://doi.org/10.2136/sssabookser5.3.c5.

S3 J. B. Goodenough, H. Y.-P. Hong and J. A. Kafalas, *Mater. Res. Bull.*, 1976, **11**, 203; https://doi.org/10.1016/0025-5408(76)90077-5.

S4 D. Novichkov, A. Trigub, E. Gerber, I. Nevolin, A. Romanchuk, P. Matveev and S. Kalmykov, *J. Synchrotron Radiat.*, 2023, **30**, 1114; https://doi.org/10.1107/S1600577523006926.

S5 B. Ravel and M. Newville, *J. Synchrotron Radiat.*, 2005, **12**, 537; https://doi.org/10.1107/S0909049505012719.